I_c Analysis of Nb_3Sn Strand Cable-In-Conduit Conductor under the Electromagnetic Force by the Structural Mechanics*)

Tsuyoshi YAGAI and Takataro HAMAJIMA[1)]

Sophia University, 7-1 Kioi-cho, Chiyoda-ku, Tokyo 102-8554, Japan
[1)]*Tohoku University, 6-6-05 Aramaki, Aoba, Sendai 980-8579, Japan*

(Received 9 December 2011 / Accepted 10 February 2012)

The Cable-In-Conduit Conductor (CICC) is the most promising one for large scale fusion magnets. Now it has been adopted as conductors for ITER magnets. Although the conductor has good mechanical strength against large electromagnetic force, the performance is not so good because the Nb_3Sn strands are fragile and the critical current density is sensitive to strain. Because the conductor is composed of hundreds or thousands of strands which are twisted and become tangled, the strands experience extra-bending during energizing magnets. It seems so difficult to analyze plastic deformation of the strands of whole conductor. Our approach to calculate it is unique in terms of using structural mechanics called "Beam Model" based on the measured strand traces inside the conduit. The calculated traces provide us the local curvatures of strands under electromagnetic force. This leads to the evaluate the conductor performance such as I_c degradation.

Keywords: cable-in-conduit conductor, Nb_3Sn strand, beam model, bending strain analysis, I_c degradation

DOI: 10.1585/pfr.7.2405026

1. Inroduction

Fusion magnets such as TF, CS coils for ITER are now under construction phase and of course no turning back. We have no question about the most suitable conductor for such large scale magnets is cable-in-conduit conductor even if some alternative conductors have been proposed [1].

The CICC is composed of hundreds or thousands of strands which is assembled of several stages of sub-cables for achieving high current density. In order to insert it into conduit for getting high mechanical strength, the twisted conductor is compressed and the void fraction would become around 35%, which leads to the tangle of strands.

According to previous reports, the strands are subjected periodic bending strain against large electromagnetic force, and the period is about 5 mm by the destructive experiment of the conductor [2]. Under electromagnetic force (EMF), the strands are free to bend between mechanical supports formed by strand-to-strand contact. This structural figure causes bending strain during operation. Besides, Nb_3Sn strand has intrinsic thermal strain after heat treatment which needs to form the superconducting filaments because the temperature difference between heat treatment and operation is around a thousand Kelvin. As for the coil operation, it is reported that strand curvature less than about 0.3% might be threshold of I_c degradation [3]. The react-and-wind type magnets would be more severe condition for the Nb_3Sn strands. In this case, the local bending strain inside the conductor would be important for evaluate the magnet performance and stability.

In our previous works, the complex strand traces which had not been revealed are measured and irregular coupling current loops are investigated by analyzing strand-to-strand contact [4, 5]. We newly develop calculation of traces under electromagnetic force based on real traces of strands by using Clapayron's three-throw moment theory [6], which provides us the continuous bending beam traces under the uniform force. This contributes to obtain local bending curves of strands and to predict the local buckling of fragile strands.

2. CICC Sample Specifications

We need actual strand traces inside conduit in advance for calculating the traces under electromagnetic force. Because the specifications of CICC and the procedure measuring the actual traces are described in previous work, the explanation of those is simplify in this paper.

The specifications of sample CICC are listed on Table 1. The sample CIC conductor consists of 81 NbTi/Cu strands of 0.823 mm in diameter without any surface coatings. In this paper, we consider the NbTi as Nb_3Sn material. The void fraction of 42% is slight higher than that of typical CICC because it is not inserted into conduit but wound by stainless steel wrap.

In order to obtain the strand traces, at first, strands are fastened by epoxy resin to avoid strand-movement on the slicing process with thickness 10 mm. Second, we measured the resistance between strand cross sections on two

author's e-mail: Tsuyoshi-yagai@sophia.ac.jp

*) This article is based on the presentation at the 21st International Toki Conference (ITC21).

Table 1 Specifications of the sample conductor.

Strand	
Strand material	NbTi / Cu
Strand Diameter	0.823 mm
Surface Coating	None
Conductor	
Construction	$3^4 = 81$
Diameter	9.73 mm
Void Fraction	42%
Twisting Pitches	65, 90, 150, 270 mm

cutting faces. If the resistance would be minimum, cross sections on both faces turn out to be identical strand. In this way, the strand positions on the faces (x-y planes) at two z positions are obtained.

3. Strand Bending Calculation

The strands are supported by adjacent strands. There are many support points along a strand and parts which are free to bend by the Lorentz force. In this case, we apply the structural beam model called Clapayron's theorem of three-moment in order to calculate the bend of the strands under electromagnetic force, which unknowns are sectional forces that we want to know directly. Comparing other methods such as slope-deflection method, the calculation is rather simple due to choosing the forces as unknowns and is appropriate for continued beams along strand axis.

Figure 1 shows the continuous beams along a wire which is applied the uniform load and expansion of three supports, where q is the uniform force whose unit is in N/m, i is the index number of support, and l_i is the length of i^{th} beam. The $\theta_{i,i-1}$ and $\theta_{i,i+1}$ illustrate the bend angle at i^{th} supporting point at left and right side of the point, respectively. According to the theory, these angles are described as follows:

$$\begin{cases} \theta_{i,i-1} = -\dfrac{1}{EI_i}\left\{\dfrac{l_i}{6}(M_{i-1}+2M_i)+B_i\right\}+R_i \\ \theta_{i,i+1} = \dfrac{1}{EI_{i+1}}\left\{\dfrac{l_{i+1}}{6}(2M_i+M_{i+1})+A_{i+1}\right\}+R_{i+1} \end{cases} \tag{1}$$

where E indicates the Young's Modulus of the wire, I_i is the geometrical moment of inertia of i^{th} beam, M_i is the bending moment at i^{th} point. The A_i, B_i are the load vector which are proportional to both q and the cube of l_i. The R_i is the tilt angle of the beam at the point depending on the supporting point depression. We take no account of it in this paper. Considering the boundary condition at the point, the angles in (1) should be identical.

$$\theta_{i,i-1} = \theta_{i,i+1} \tag{2}$$

We get the following equation with (1) and (2).

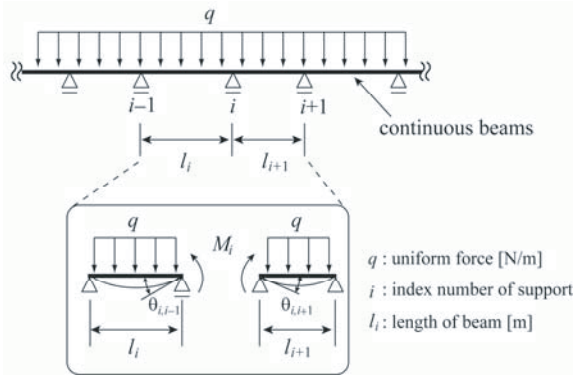

Fig. 1 Schematic drawing of the Clapayron's theorem of three-moment.

$$\begin{aligned} &\frac{l_i}{I_i}M_{i-1}+2\left(\frac{l_i}{I_i}+\frac{l_{i+1}}{I_{i+1}}\right)M_i+\frac{l_{i+1}}{I_{i+1}}M_{i+1} \\ &\quad=-6\left(\frac{B_i}{I_i}+\frac{A_{i+1}}{I_{i+1}}\right)+6E(R_i-R_{i+1}) \end{aligned} \tag{3}$$

This is the Clapayron's three-throw moment relation which consists of adjacent three supporting points [6].

The strand deflection is calculated by using bending moment which would be obtained by solving simultaneous equation (3). The deflection is calculated by following differential equation:

$$\frac{\partial^2 y}{\partial x^2} = -\frac{M}{EI} \tag{4}$$

By double integration of (4), the deflection must be obtained. Integral constants are determined by taking into consideration the initial traces. In this paper, we use 5 GPa Young's Modulus [7].

4. Calculation Procedure

Before explaining the procedure, we would introduce some assumptions for calculation. First, it is shown in Fig. 2 (a) that the strand-to-strand contact which can be taken as a supporting point against load. When a load would be applied top-to-bottom (in this paper, -y direction), the angle between the line whose ends are the centers of those strands and y axis should be less than 60 degree. Although the threshold has no physical background, it seems sufficiently be reasonable. In order to simplify the calculation, we never consider the friction force on the strand surface. Second, Fig. 2 (b) shows the increment of support point along the way of applying EMF. During bending, the beam could be get in touch with other strands or conduit. If the contact condition meets the assumption mentioned above, the contact would be taken as a new support against EMF.

Figure 3 shows the flow chart of the strand bending calculation. First of all, we extract the beams which suffuse the assumptions mentioned above by using measured traces of sample CICC. Second, the strand traces are calculated by using (3) and (4) as a function of the load. Third,

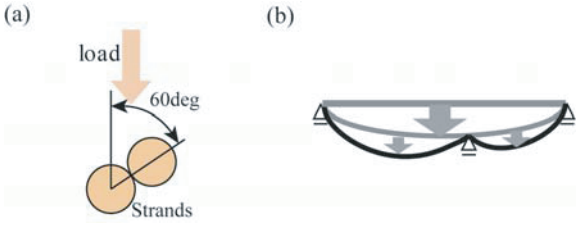

Fig. 2 Schematic views of the strand-to-strand contact.

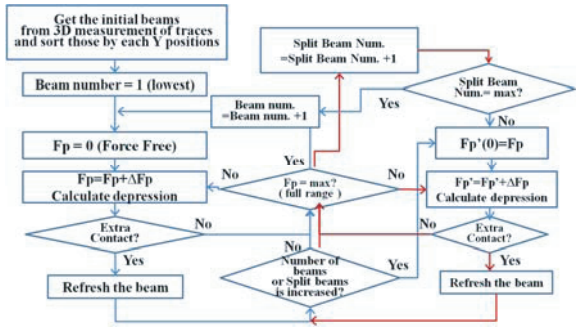

Fig. 3 Flow chart of the strand bending calculation. The increment of number of beams is considered by recursive calculation.

the beams are sorted by the average heights of those. Because bending should be occur in order from bottom to top part of the CICC, we repeat the calculation which will be explained in following part from the underlying beams. The operating procedure of the electromagnetic force is as follows:

(1) ΔFp, a piece of force is applied to the selected beam.

(2) If new contacts are obtained by the strand deflection, the new trace which is a function of the force is calculated throughout the strand involve the beam.

(3) If the force is fully applied at all divided beams, the procedure is applied to the next beam. The simultaneous equations with literal expressions are solved by using the programming language MATLAB.

5. Results and Discussion

In CICC, there are huge number of tangles of strands. Because the strands are supported by adjacent ones, the beams are formed between a pair of supporting points. Therefore, the length of beam is determined by the distance between two supporting points. The destructive examination indicated that the typical interval of the points was about 5 mm [2]. Figure 4 shows the beam length distribution derived from measured strand traces. Actually, the majority of lengths of beams is about 5 mm, however, there are not a few beams which length exceeds 10 mm. Y. Nunoya *et al.*, investigated experimentally that the periodic bending strain would cause the I_c degradation of Nb_3Sn strands. Their discussion about the disagreement

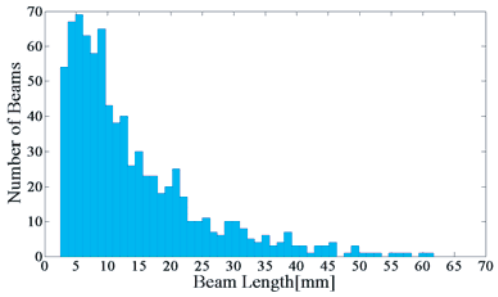

Fig. 4 The histogram of beam length distribution.

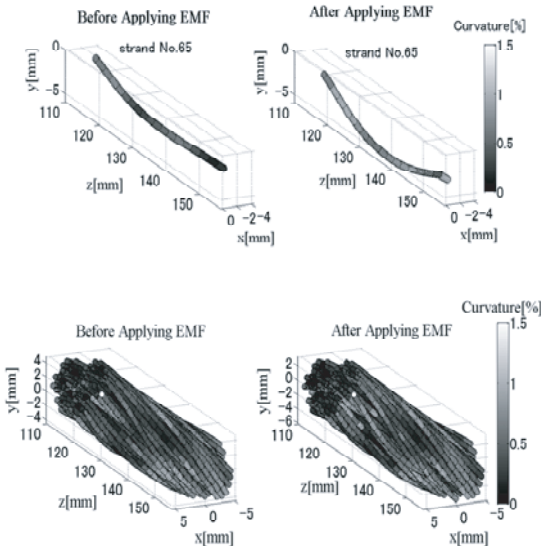

Fig. 5 3-dimensinal plot of the strand trace No. 65 (upper) and the all traces (lower). The contrasting density indicates the curvature.

between experiment and calculation pointed out the bad effect of simple assumption [8]. We think it is necessary to introduce the precise information about beams. In this paper, the EMF is less than 1620 N/m and the conductor length is limited to 260 mm because of saving CPU time. Figure 5 shows the 3-dimensional strand traces before (left side) and after (right side) applying EMF. The plots on the lower side indicate all strand traces, and upper side the trace of strand No. 65. It is shown that the trace is bent downward corresponding to the EMF direction. In this case, the displacement is about 2 mm and the absolute curvature locally reaches 1.8% displaced from virgin state. It is noticed that the average of them through the strand axis should be much smaller than the local ones. The maximum average curvature is about 0.35%. The overall average curvature is less than 0.1%, which seems to have no relation to the reduction of conductor performance.

Figure 6 shows the relation between curvatures and beam length. According to the beam model, the strain (i.e. curvature of strands) depends on the following equation

$$\text{Strain} = \frac{24 r_f y}{l^2} \tag{5}$$

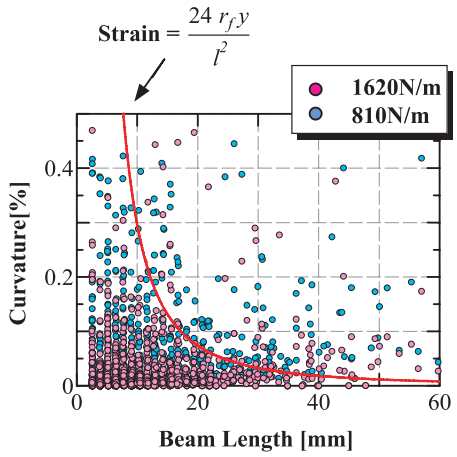

Fig. 6 The relation between beam length and the strand curvature. The curve indicates the theoretical one formulated by beam model.

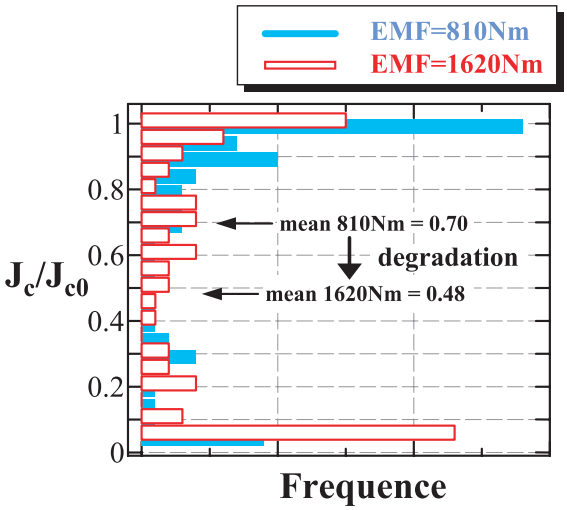

Fig. 7 The J_c degradation profile for 81 strands.

where r_f, y and l indicates radius of filament region, displacement and beam length, respectively. By using the average displacement of 0.03 mm, the strain characteristic would be described as a red curve in Fig. 6. This curve well represents the feature of the beam length dependence of the curvatures.

Although the overall average of strand curvature might not affect to the conductor performance, now we mention the average over each strand as a parameter affected to the critical current density of each strand. Figure 7 describes the J_c profile for each strands. According to the [8], 0.8% curvature means 50% degradation of I_c. Then, we assume the curvature dependence of J_c should be the following function,

$$J_c = J_{c0}\left((1 + 0.08 \times x^2) \times \exp(-Dx^2)\right), \quad D = 1.11 \tag{6}$$

where J_{c0}, is the current density without curvature. As the EMF increases 810 Nm to 1620 Nm, the number of robust strands (J_c/J_{c0} is around 1) is decreased and that of degraded strands (J_c/J_{c0} is around 0) is increased. Therefore, the average of the ratio over the strands drops as the EMF increase.

6. Summary

We calculated the strand traces and curvatures under EMF by using structural mechanics based on the measured traces. The local curvature would be about 2%, while the overall average value was less than 0.1%. The I_c degradations of strands are different from each other, and the average of critical current density ratio might depends on the EMF. Due to the strand curvature, it is indicated by our estimation that there might be strongly degraded strands inside the conduit, and inter-strand current sharing would be important for the conductor stability under the EMF.

[1] N. Koizumi *et al.*, Cryogenics **42**, 675 (2002).
[2] P. Bruzzone *et al.*, IEEE Trans. Appl. Supercond. **13**, no.2, 1452 (2003).
[3] B.J. Senkowicz *et al.*, IEEE Trans. Appl. Supercond. **15**, no.2, 3470 (2005).
[4] T. Yagai *et al.*, IEEE Trans. Appl. Supcercond. **19**, no.3, 2387 (2009).
[5] T. Yagai, Cryogenics **50**, 200 (2010).
[6] H. Miyamoto, *Structural Mechanics* (Gihodo Press, 2007).
[7] L. Chiesa, *doctoral thesis*, MIT, 2006.
[8] Y. Nunoya *et al.*, IEEE Trans. Appl. Supcercond. **14**, no.2, 1468 (2004).